

GODDARD SPACE FLIGHT CENTER

Evaluation Report

"The information contained herein is presented for guidance of employees of the Goddard Space Flight Center. It may be altered, revised, or rescinded due to subsequent developments or additional test results. These changes could be communicated internally by other Goddard publications. Notice is hereby given that this document is distributed outside of Goddard as a courtesy only to other government agencies and contractors and is understood to be only advisory in nature. Neither the United States Government nor any person acting on behalf of the United States Government assumes any liability resulting from the use of the information contained herein."

Microcircuit (8)
Mfr.: Analog Devices
P/N: AD6640
D/C: 9951

Malfunction Report

Purchase Specifications
commercial

Incoming Inspected

Screening Specifications
commercial

Project

VCL

System

Parts testing

Requester

K.Sahu (562)

Initiated Date

6/01/00

Investigator

A.Teverovsky (300.1)

Approval for Distribution/Date

Background

Eight Analog Devices AD6640 commercial microcircuits intended for the VCL project, L/I # VCL086F, were submitted to the GSFC Parts Analysis Laboratory for evaluation of their design, materials and potential risk for long term reliability.

Part Description

The AD6640 is a high-speed, low-power monolithic 12-bit analog-to-digital converter. The die is attached to the silver-plated copper lead frame using a silver epoxy and is interconnected to the leads with 1.2 mil gold wires. The part is encapsulated in a standard surface mount 44-terminal plastic thin quad flat package (TQFP, type ST-44).

The part is designed using a high-speed complementary bipolar process, called XFCB (eXtra-Fast Complementary Bipolar). The XFCB is a variation of the SOI technology which employs bonded wafers with deep trenches to achieve full dielectric isolation. This process has been in production by Analog Devices for more than 6 years. The major advantages of such an isolation scheme are to provide radiation hardening to the device, improve slew rate, increase packing density, reduce cross-talk and die size, and eliminate latch-up.

Analysis

1. External and Radiographic Examinations.

All samples were serialized (from SN 101 to SN 108) and subjected to external microscopic examination and radiography. Figure 1 gives an overall view of the part. Typical top and side X-ray views are shown Figure 2.

No package warping, cracks, voids, or foreign inclusions in the plastic encapsulant were observed. No gaps were observed between the entry of the leads and the molding compound. Radiographic examination showed adequate wire bond dressing. The die-paddle and the leads had lead lock holes which enhanced a bond between the molding compound and the lead frame and increased moisture resistance of the part.

The between-leads space near the package in all parts was filled with the oozed molding compound (mold flash). Figure 3 shows a typical view of the mold flash. The oozed compound forms a thin layer which could be relatively easily broken during mounting of the microcircuits on the board. This might contaminate the board with polymer particles.

2. Scanning Acoustic Microscopy. Reflow simulation.

Top and bottom sides of all parts were examined using an acoustic microscope (C-SAM mode with a 15 MHz transducer) before and after reflow and solder heat resistance simulation.

Reflow simulation.

To simulate surface mounting technology (SMT) conditions, eight parts were passed through the CENTECH vapor phase reflow machine three times. The preheat time and temperature were 60 s and 125 °C and the reflow time and temperature were 40 s and 220 °C.

Solder heat resistance.

Two parts (SN 107 and SN 108) after reflow simulation were immersed in a solder pot at 245 ± 5 °C for 5 seconds and then spray cleaned with isopropanol. This cycle was repeated three times.

C-SAM Examination Results.

External visual examination did not reveal any defects. C-SAM examination showed that all parts had similar acoustic images (see Figures 4 and 5). No abnormalities at the die-molding compound interface or any other interfaces were noticed.

3. Internal Examinations.

Two samples were decapsulated in red fuming nitric acid and examined microscopically. Figure 6 shows an overall view of the part after decapsulation and Figure 7 illustrates typical views of metallization patterning. No abnormalities were found except for somewhat large grains of aluminum metallization. The identification marking on the dice was "BCOM, 1997, 6640-R2".

4. Bond Pull Test.

All 44 wires in one sample were subjected to wire pull testing. The part passed the test according to the formal criteria of MIL-STD-883, TM 2011 (2.5 g-f for 1.2 mil gold wires). The average bond pull force was 7.96 g-f with a standard deviation of 0.82 g-f. The range of the pull strength was from 6.3 g-f to 9.7 g-f.

5. SEM examination of glassivation and wire bonds.

Bonds and glassivation in two samples were inspected using a SEM. No glassivation or bonding defects were found (see Figures 8 and 9). Energy-dispersive X-ray microanalysis (EDX) indicated that the glassivation was composed of a nitride film overlaying a silicon oxide film.

6. Glassivation integrity.

This examination was performed on one sample per MIL-STD-883D, Method 2021, "Glassivation layer integrity". The test involved a high-power optical examination after the die was subjected to aluminum etch. Aluminum etching did not reveal any cracks or other defects in the glassivation.

7. SEM inspection of metallization.

The metallization was inspected in one sample per MIL-STD-883D, Method 2018 after glassivation removal. The part is designed with two aluminum metallization levels. No patterning problems, misalignment, or other defects were found in either the top or the bottom metallization layers. The first level of metallization employs a thin Ti/W barrier layer. The part has adequate planarization which significantly reduced the step coverage problem. Figure 10 shows details of the metallization system.

SEM examination confirmed large grain size in the aluminum metallization and revealed defects which appeared to be intergranular cracks (see Figure 11). However, metallization grains are known to be preferred locations for chemical attack and the observed defects are artifacts caused by SiO₂ wet etching. Large grain size increases conductor life at high current densities by reducing the risk of electromigration failures. Considering the good protection characteristics of the used glassivation system and the fact that the part is not intended for operation in moist environment, the large grain size of the metallization most likely will not compromise the reliability of the part.

8. Package-level Cross Sectional Examinations.

Sample SN 107 was cross-sectioned and examined at several planes and interfaces between the molding compound and the die assembly were examined using a high power optical microscope and a SEM.

The molding compound had no cracks or voids and formed intimate contact to all internal surfaces (die, wires, and lead frame). No delaminations between the glassivation and the molding compound were observed. Although crevices at the lead entry to the package are a common defect in plastic encapsulated microcircuits, the cross sectioning showed that the leads in these parts were completely embedded in the molding compound without any gaps at their entry (see Figure 12).

The lead frame was made of copper of approximately 150 μm thick. Finger tips and the top and the sidewall of the die paddle were locally spot-plated with silver (approximately 7 μm thick). External parts of the lead frame were tinned.

The gold wires formed metallurgical contacts with the silver plating at all examined wire-to-lead frame bonds (see Figure 13). Ball bond cross sectioning showed the formation of an adequate Au/Al intermetallic layer of 2 - 3 μm in thickness (see Figure 14).

The die was mounted to the lead frame base with a thin layer of silver epoxy. The silver filler was uniformly distributed along the adhesive layer. A minor delamination at the silver epoxy-to-paddle interface (see Figure 15) is common for similar designs and does not pose any reliability risk.

9. Die-level Cross Sectional Examinations.

Figure 16 shows typical cross sections of the die. The part is designed using a relatively thick buried oxide and silicon film (1.2 μm and 4.5 μm respectively). This is typical for the bond and etch-back SOI technology and provides better insulation and quality of the active silicon layer compared to the SIMOX process.

SEM examination of the die cross-sections did not reveal any defects in the dielectric trench or lateral isolation and/or in the metallization system.

Conclusions.

1. The Analog Devices AD6640 is designed using a variation of SOI technology which is beneficial for precision high-speed A/D converters, provides radiation hardening to the part and eliminates the possibility of latch-up failures.
2. The die manufacturing was satisfactory. No defects were found in the glassivation, and the metallization exhibited good planarization, alignment and uniformity.
3. The wire bonding exhibited normal alignment, dressing, strength and deformation of the ball and stitch bonds. The stitch bond made metallurgical contact to the silver-plated lead fingertips and the ball bond formed an adequate Au/Al intermetallic at the die contact pad.

4. Cross sectioning indicated good integrity of the part. The molding compound formed intimate contact to the leads and to all elements of the die-lead frame assembly. Some delamination at the paddle-to-silver epoxy interface most likely will not pose any reliability risk and can be considered minor.
5. SMT simulation did not cause any delaminations at the die-to-molding compound interface and/or cracking in the package.
6. The evaluation confirmed the adequacy of the fabrication process and quality control for the Analog Devices AD6640 microcircuit. No serious reliability problems were found.

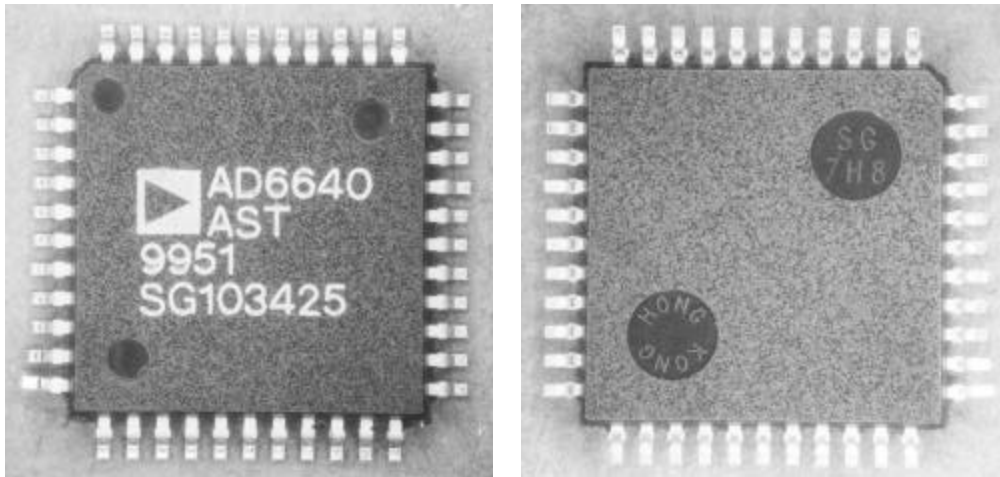


Figure 1. Top and bottom views of the part.

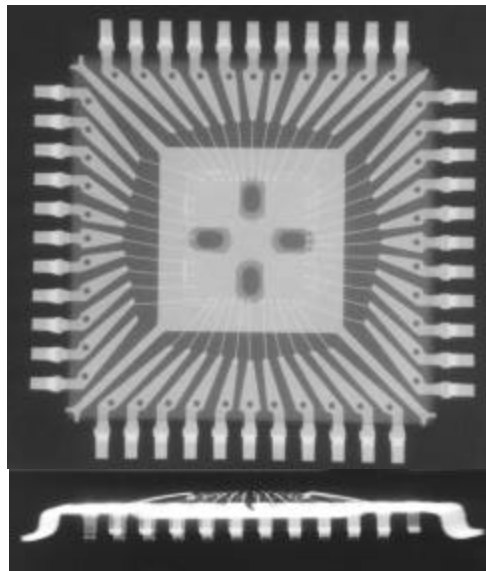


Figure 2. Top and side radiographic views of the part showing adequate lead frame design, wire dressing and layout.

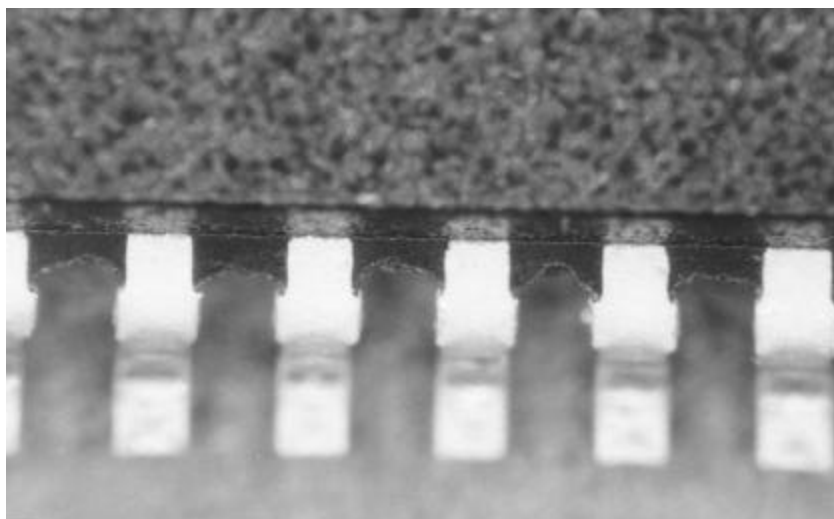


Figure 3. Mold flash between the lead entries.

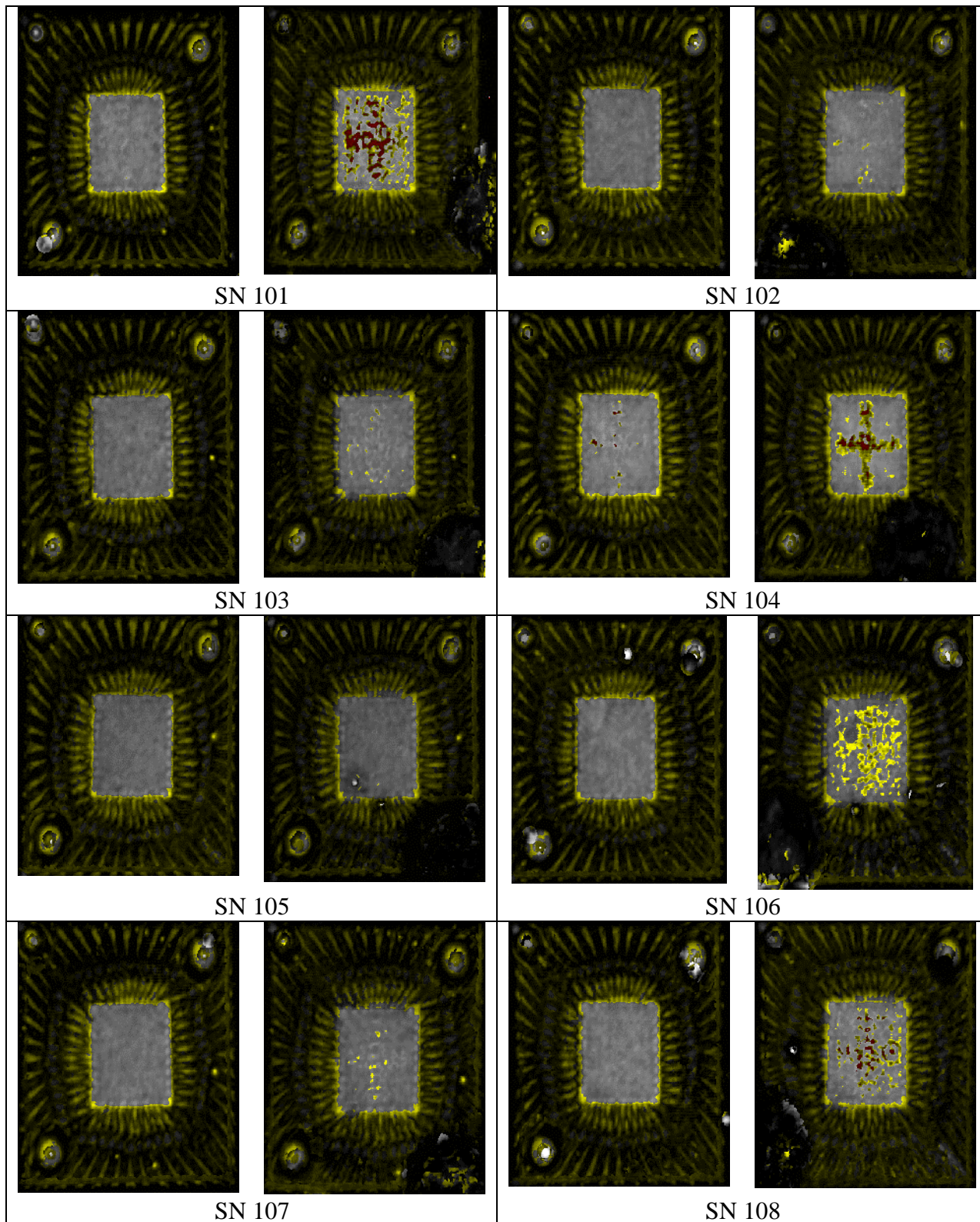


Figure 4. Initial (left) and post-SMT simulation (right) acoustic images. Top views.

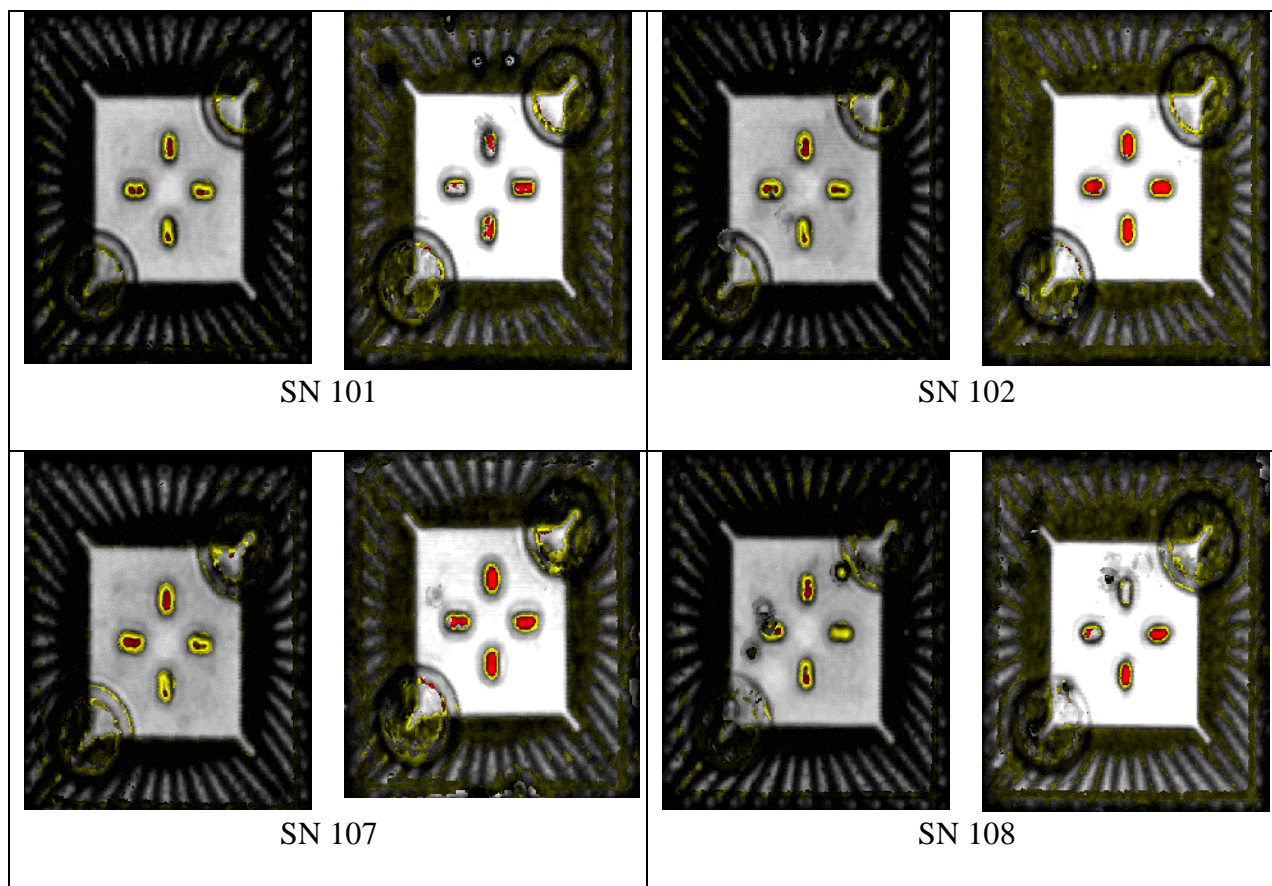


Figure 5. Initial (left) and post-SMT simulation (right) acoustic images. Back views.

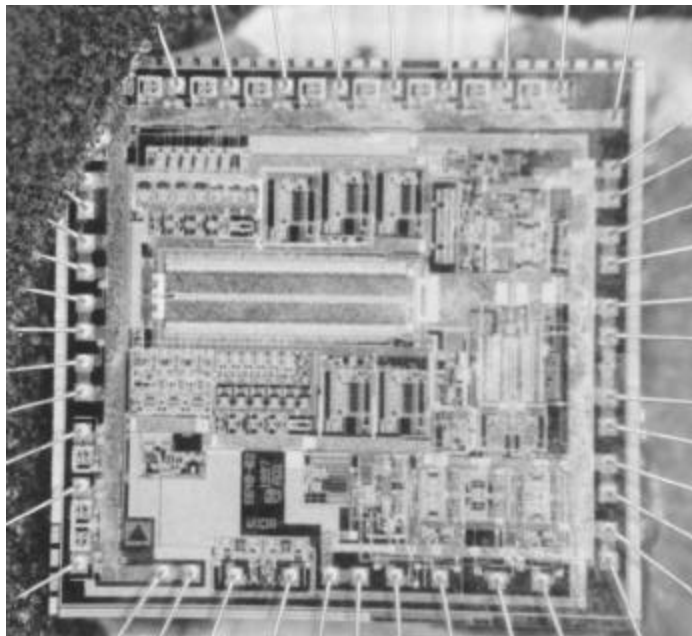


Figure 6. Overall view of the die after decapsulation.

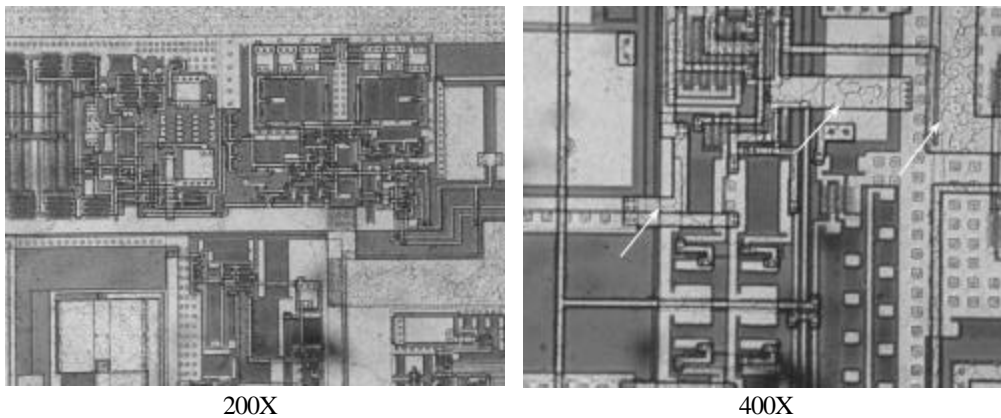


Figure 7. Optical views showing the large metallization grains.

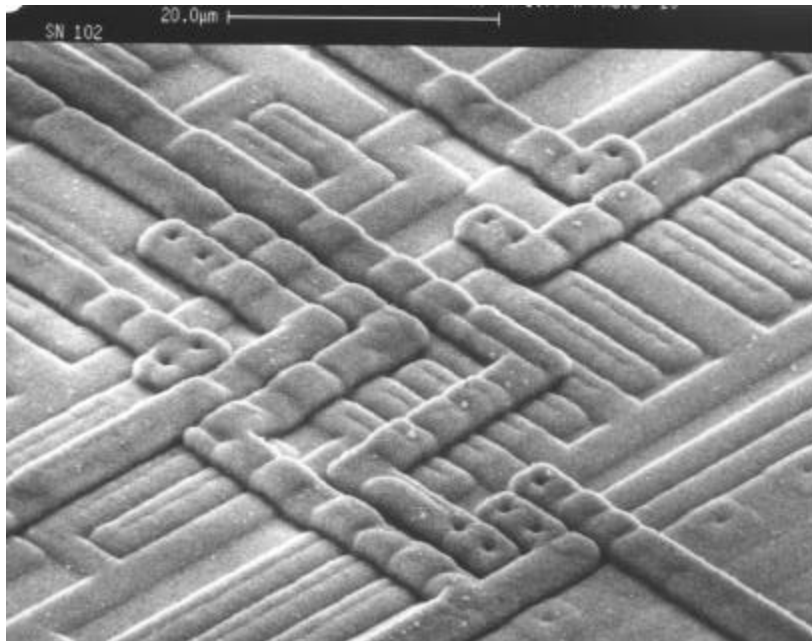


Figure 8. SEM view of the glassivation showing good coverage over metallization.

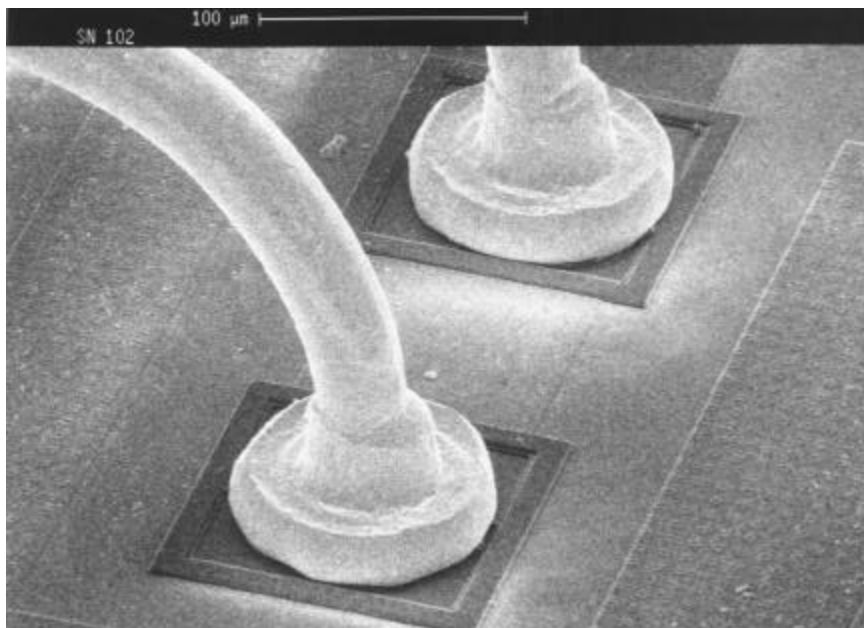


Figure 9. Typical gold wire bonds show acceptable deformation and placement.

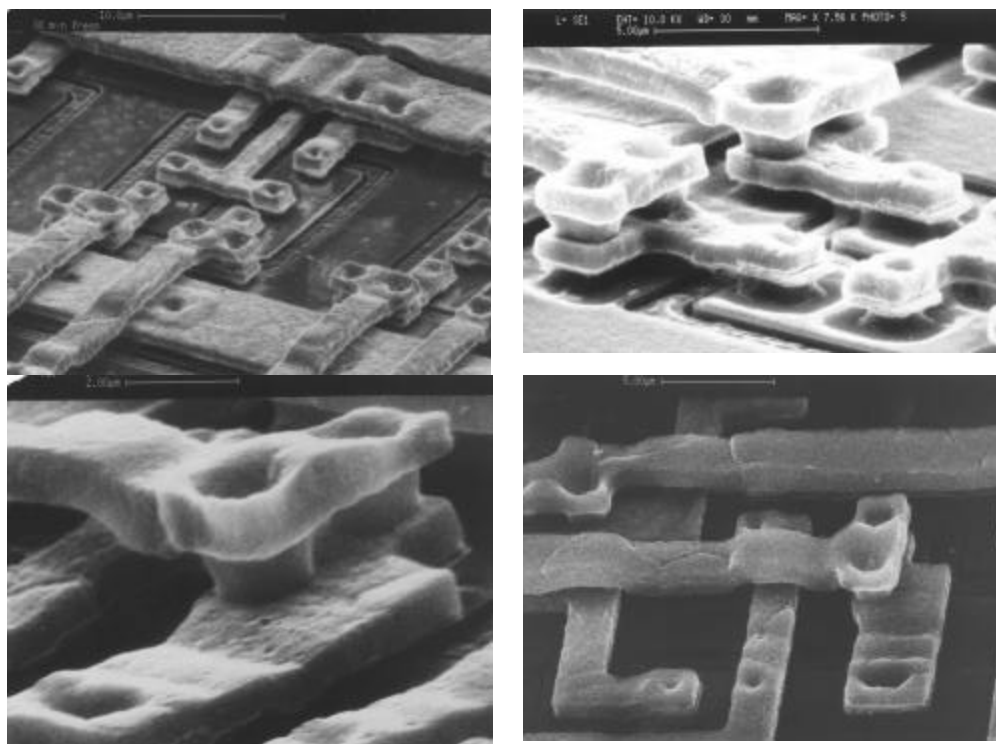


Figure 10. SEM views of the first and second levels of aluminum metallization showing good alignment.

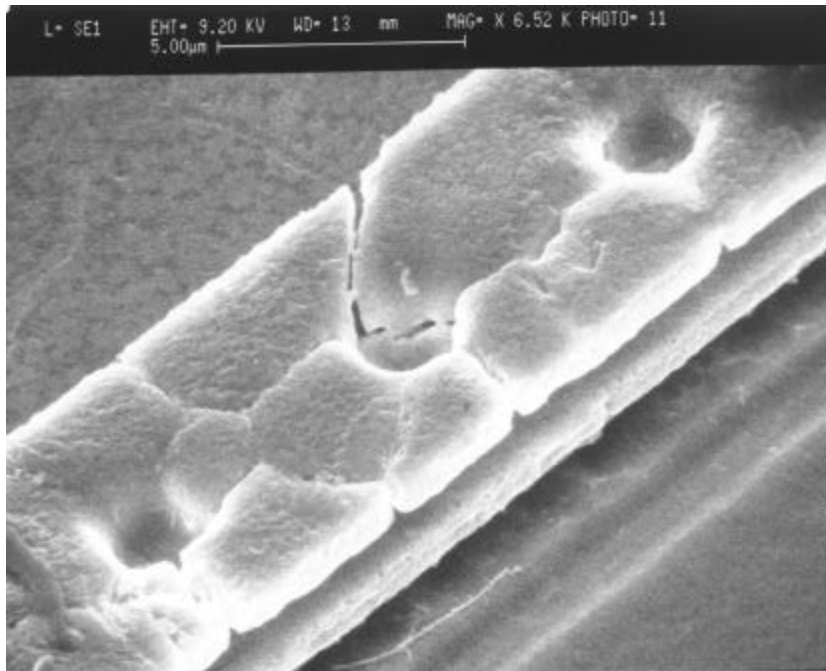


Figure 11. Aluminum run fractured along the boundary grains.

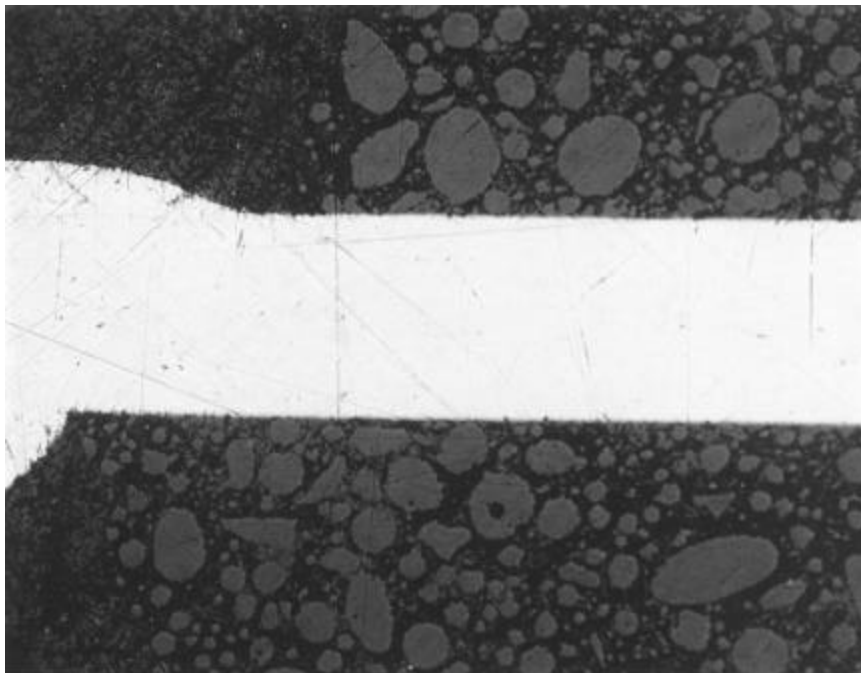


Figure 12. Cross section of the lead entry.

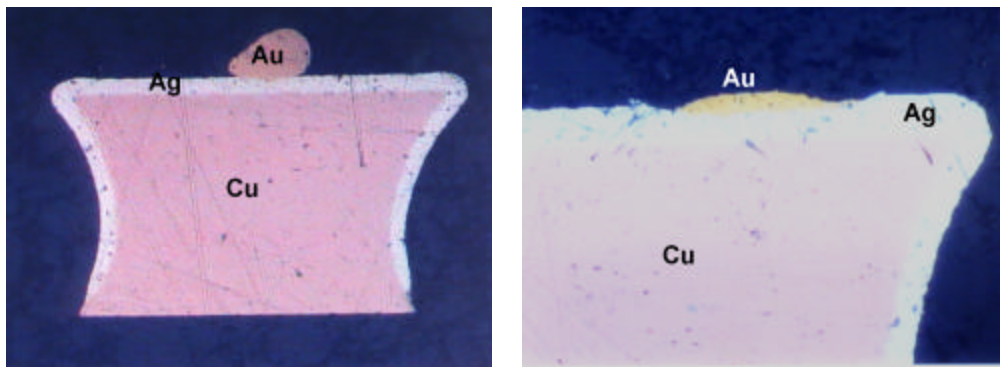


Figure 13. Stitch wire bond to the lead.

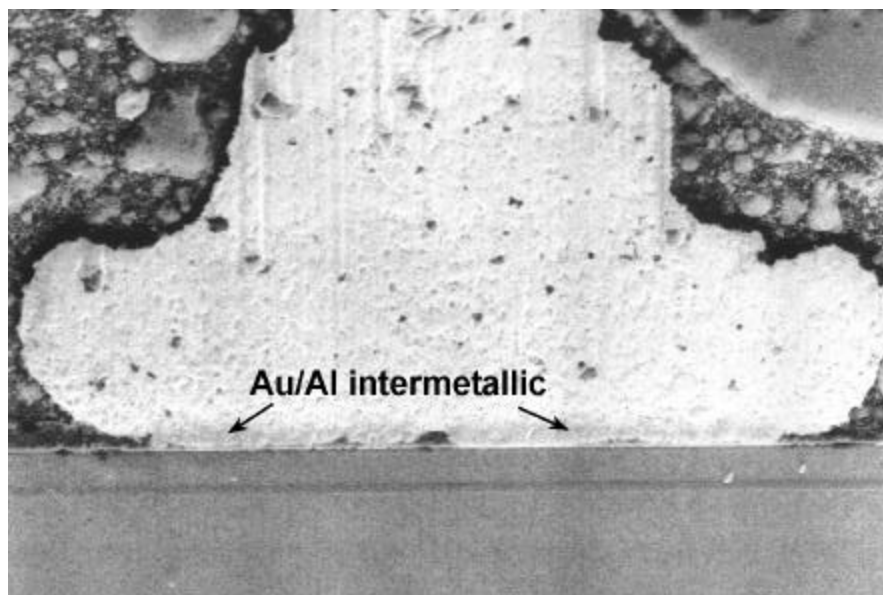


Figure 14. Cross section of the wire bond showing adequate Au/Al intermetallic formation.

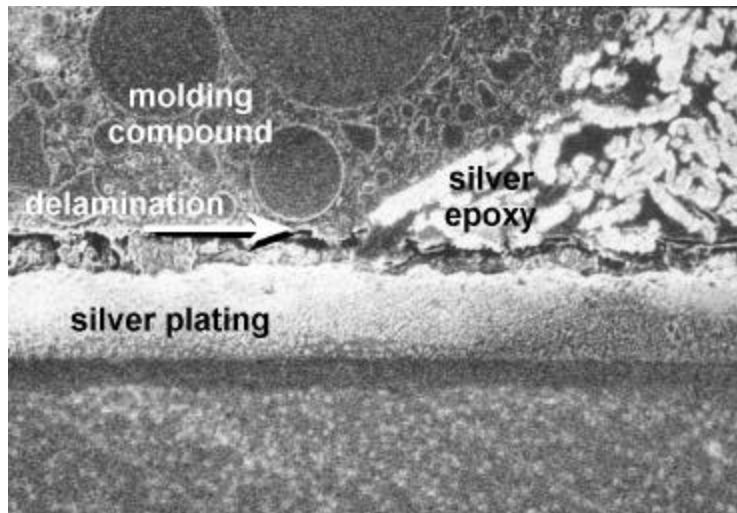


Figure 15. Delamination along the top of the lead frame paddle.

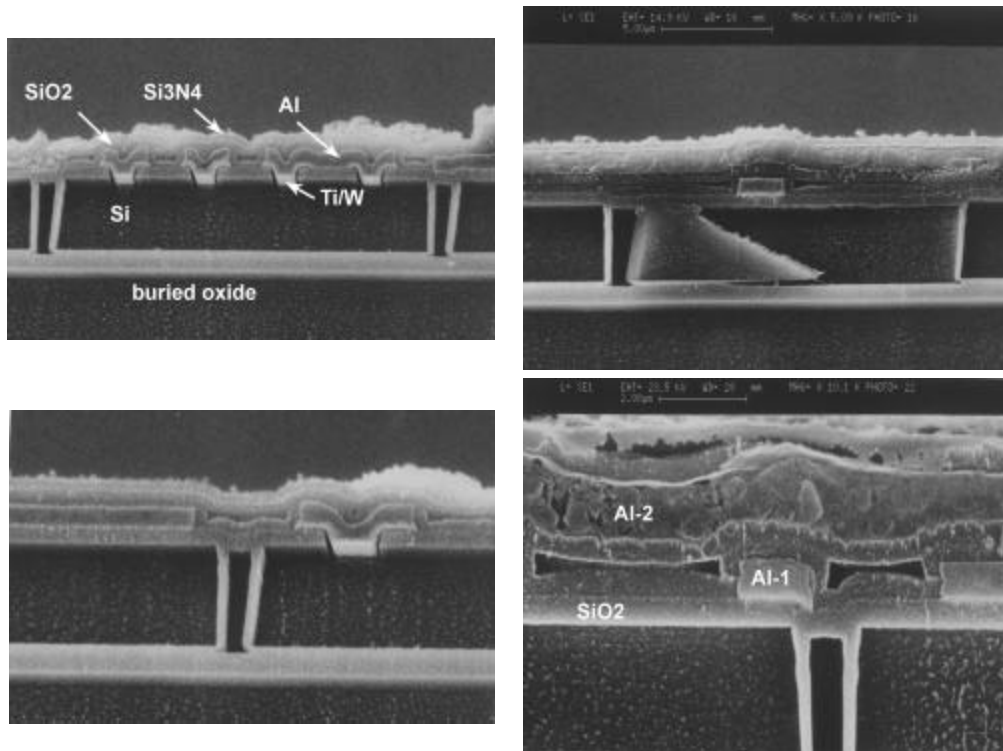


Figure 16. Cross-section views of the die showing buried oxide and silicon active areas. Note adequate step coverage of the passivation layer.